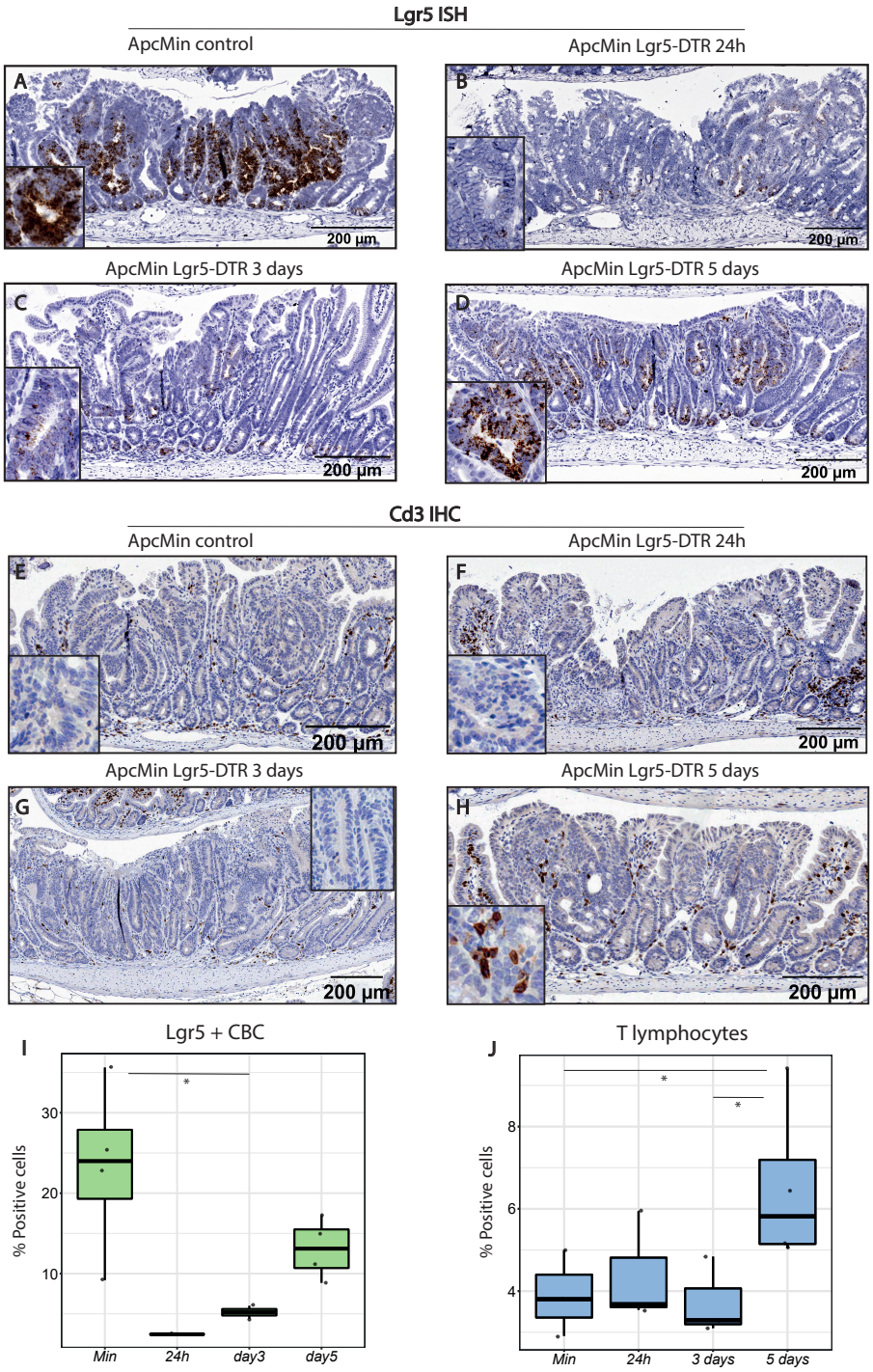

Figure 40: CBC ablation in APC^{Min} mice drives a subtle T cell infiltration. A-H. ISH for *Lgr5* and IHC for Cd3 in polyps from APC^{Min} control (A,E) and APC^{Min}-$Lgr5^{DTR}$ animals 1 (B,F), 3 (C,G) and 5 days (D,H) after DT administration. I,J. Image quantification of the levels of *Lgr5+* (I) and Cd3+ (J) cells in polyps from APC^{Min} control (A) and APC^{Min}-$Lgr5^{DTR}$ animals 1 (B), 3 (C) and 5 days (D) after DT administration. Significance was assessed using a pairwise t-test and p.value was adjusted using the Holm method. Asterisks indicate a p-value <0.05 (*), <0.01(**) or <0.001 (***).

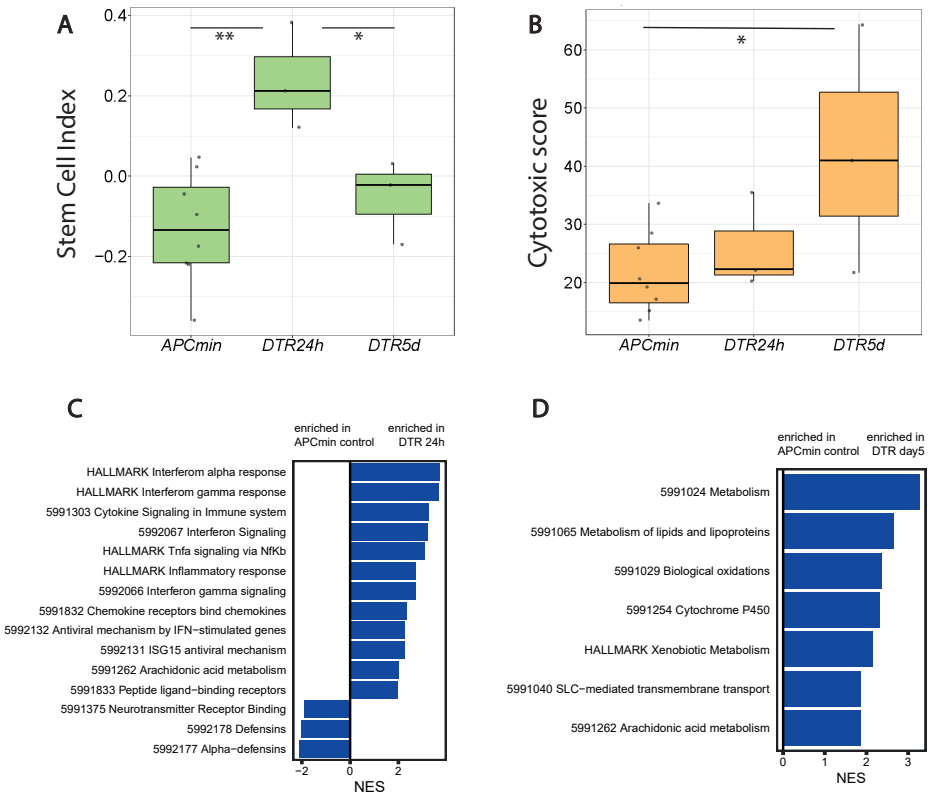

Figure 41: Transcriptomic changes driven by the CBC ablation from APC^{Min}-$Lgr5^{DTR}$ polyps. A,B. Gene Set Variation Analysis (GSVA) scores for a Lgr5[7] signature (A) and Cytotoxic Score[247] (B) from APC^{Min}-$Lgr5^{DTR}$ polyps 24h and 5 days post-CBC ablation. C,D. Differentially Expressed pathway between controls and APC^{Min}-$Lgr5^{DTR}$ polyps 24h (C) or 5 days (D) post-CBC ablation. For GSVA and Cytotoxic scores, statistical significance was assessed using a pairwise t-test and p.value was adjusted using the Holm method. For GSEA, pathways were ranked by Negative normalized Enrichment Score. Statistical differences were assessed by the fast algorithm[232] and significance threshold was set at an adjusted p.value < 0.05. Asterisks indicate a p-value <0.05 (*), <0.01(**) or <0.001 (***).

Furthermore, the numbers of Caspase-3+ cells increased significantly in APC^{Min}-$Lgr5^{DTR}$ crypts and polyps 24h after DT administration (Fig.42D,I), indicating that Lgr5+ cells were dying by apoptosis. Indeed, RNAseq data showed an upregulation of an apoptosis gene signature 1 day post-injection (Fig.42J). However, Caspase-3 staining and apoptosis scores returned to basal levels by day5 (Fig.42).

Overall, Lgr5+ cell ablation had a minimal impact on the immune landscape of APC^{Min} animals, suggesting that it is not an expansion of the CBC SC themselves

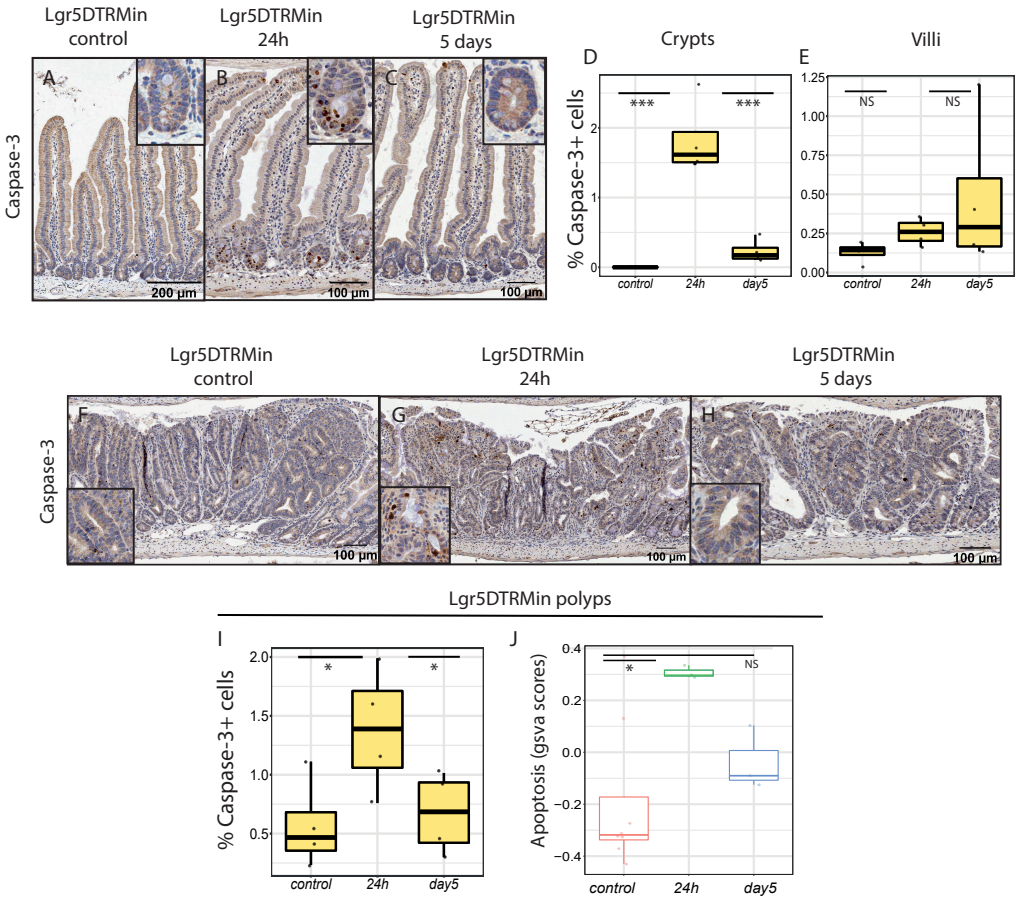

Figure 42: Administration of Diphteria Toxin (DT) to APC^{Min}-$Lgr5^{DTR}$ animals causes CBC to die by apoptosis. A-C, F-H. IHC for the apoptosis marker Caspase-3 in untransformed tissue (A-C) and polyps (F-H) from control and APC^{Min}-$Lgr5^{DTR}$ animals 24h and 5 days after DT administration. D,E,I Image quantification of the levels of Cd3+ cells in crypts (D), villi (E) and polyps (I) of controls and APC^{Min}-$Lgr5^{DTR}$ animals 24h and 5 days after DT administration. J. Apoptosis GSVA scores in control and APC^{Min}-$Lgr5^{DTR}$ animals 24h and 5 days after DT administration. Statistical significance was assessed using a pairwise t-test and p.value was adjusted using the Holm method. Asterisks indicate a p-value <0.05 (*), <0.01(**) or <0.001 (***)

that is responsible for the immune exclusion observed in Wnt disrupted polyps.

5.8 Porcupine Inhibition Prevents Rspo3-induced Polyposis and Improves Survival of *Lgr5-Rspo3* Animals

After disproving that immune evasion was restricted to CBC cells, the next step was to test the direct link between WNT activation and T cell exclusion. To do that, an experimental setting that would allow for WNT activation to be abruptly altered was needed. Porcupine inhibitors are a well established experimental WNT inhibitors that can efficiently block this pathway in ligand-dependent models of WNT-driven polyposis. Here, a non-commercial Porcupine inhibitor (RXC004, Redex) and the *Lgr5-Rspo3* model were used to investigate whether pharmacological blockage of Wnt signals could revert the immune exclusion phenotype.

Given that the *Lgr5-Rspo3* mice do not have mutations downstream the Frizzled receptor, and that WNT activation is a pre-requisite of Rspo3-driven transformation[24], effective Wnt ligand inhibition should revert the polyposis observed in this model. Previous experiments by Redex demonstrated that a dose of 5mg/kg was well tolerated in ligand-independent models of WNT-driven colorectal transformation. Based on this, *Lgr5-Rspo3* animals were gavaged with 5mg/kg of RXC004 on a regime of 5 days on, 2 days off. Unexpectedly, treated animals developed signs of pathology within a week, which included anaemia, hunching and lack of activity. In addition, their weighs dropped >15%. Consequently, animals were sacrificed and samples were collected. H&E staining of the intestines revealed the absence of crypts throughout the small bowel (Fig.43C,D). Moreover, brown ISH for *Lgr5* showed a complete lack of Lgr5+ cells within the crypt-villus axis (Fig.43F). Based on this evidence, it was hypothesized that the absence of intestinal progenitors might be driving collapse of the crypt base columnar stem cell population. Interestingly, WT controls treated with the same dose of RXC004 lost CBC cells but retained functioning crypts and animals tolerated the dose without significant morbidity (Fig.43A,B). Collectively, this indicates that the *Lgr5-Rspo3* animals may have a higher sensitivity to Wnt inhibition than WT mice.

In order to find a concentration of RXC004 which could revert the Rspo3-induced phenotype without causing life-threatening side effects, a dose-response experiment was conducted. This time, animals were treated for a total of 5 days with doses ranging from 0.5mg/kg to 5mg/kg, and collected on day 7. ISH for *Lgr5* revealed a dose-dependent reduction in the number of Lgr5+ cells within the crypts of treated *Lgr5-Rspo3* mice (Fig.43E-L). Indeed, the original dose had to be reduced by 1/5 for

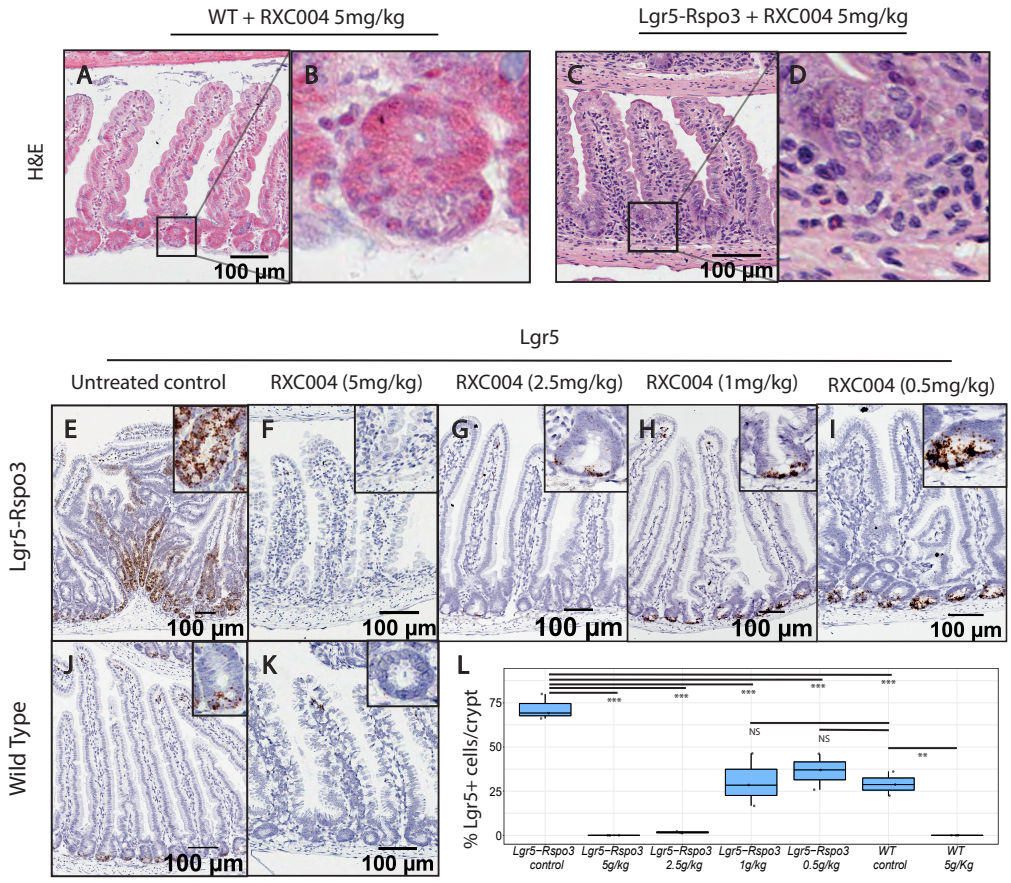

Figure 43: High doses of RXC004 cause CBC ablation and intestinal collapse in *Lgr5-Rspo3* animals. A,B. H&E of intestines from WT (A) and *Lgr5-Rspo3* (B) animals treated with 5g/kg of RXC004. C-I. ISH for *Lgr5* in *Lgr5-Rspo3* (C-G) and WT (H,I) animals treated with RXC004. J. Quantification of the levels of *Lgr5* in *Lgr5-Rspo3* and WT animals treated with RXC004. Statistical significance was assessed using a pairwise t-test and p.value was adjusted using the Holm method. Asterisks indicate a p-value <0.05 (*), <0.01(**) or <0.001 (***)

animals to have normal levels of Lgr5+ cells while reverting Rspo3-driven hyperplasia. Based on these results, a dose of 1mg/kg was chosen for consequent experiments.

Once the dose of RXC004 had been decided upon, *Lgr5-Rspo3* animals were gavaged with 1mg/kg of RXC004 on a regime of 5 days on, 2 days off. Animals were collected when they showed signs of pathology or on the day of the 28th dose (the last one permitted per license). Unlike in the previous experiment, RXC004-treated animals tended to have longer life-spans than their vehicle-treated counterparts (Fig.44C), although these differences were slightly below statistical significance. Moreover, histopathological assessment of treated samples showed an almost complete

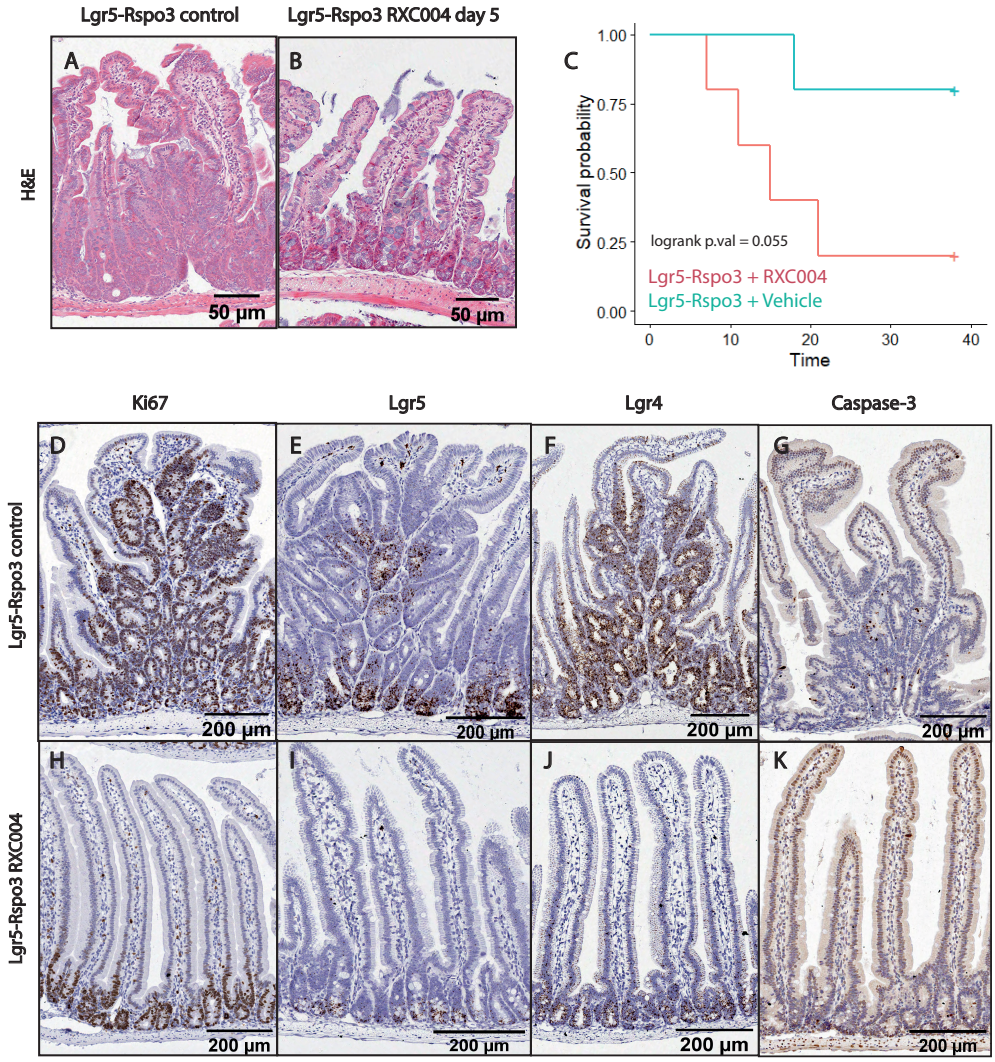

Figure 44: Treatment with a Porcupine inhibitor reverts polyposis in *Lgr5-Rspo3* animals. A,B. H&E of intestines from *Lgr5-Rspo3* treated with vehicle (A) or 1g/kg of RXC004 (B). C. Kaplan-Meier comparing the survival of *Lgr5-Rspo3* animals treated with vehicle and 1g/kg of RXC004. Statistical differences were tested using a logrank test. D-K. ICH for Ki67 (D,H), Caspase-3 (G-K) and ISH for *Lgr5* (E,I), *Lgr4* (F,J) in intestines from *Lgr5-Rspo3* injected with vehicle (D-G) or treated with 1g/kg of RXC004 (H-K).

reversion of the hyperplastic and polyposis phenotype induced by *Rspo3* overexpression (Fig.44A,B). In addition, these animals experiences a clear reduction of *Lgr5+* and Ki67+ cells and their expression of Lgr4 was reminiscent of WT intestines. Furthermore, caspase-3 staining revealed no signs of apoptosis in *Lgr5-Rspo3* treated animals at the time of collection (Fig.44D-K). Overall, these results prove that RXC004

treatment can revert to a great extend the polyposis phenotype induced by R-spondin 3 overexpression without compromising the viability of *Lgr5-Rspo3* animals.

5.9 Porcupine Inhibition can Revert Immune Exclusion from *Lgr5-Rspo3* ECFs, but not Conventional Crypts

Once the effectiveness of RXC004 had been assessed, the effect of acute abrogation of WNT signalling on the immune compartment of Lgr5-Rspo3 polyps was investigated. To do that, *Lgr5-Rspo3* animals were daily gavage with RXC004 and samples were collected on day 2, 3, 4 and 5. A comprehensive assessment of H&E intestinal sections revealed that the phenotype of *Lgr5-Rspo3* animals had been almost completely reverted within 5 days (Fig.45A,B). Furthermore, IHC for Cd3 showed signs of T cell infiltration within the ECF of RXC004-treated animals, but not conventional crypts (Fig.45C-F). Indeed, quantification of these stains revealed a steady decrease in the number of ECF and an increase in the percentage of Cd3+ cells within ECF from day 0 to 5 (Fig.45G,H).

In order to characterize the lymphocytic infiltrate within ECF, samples were stained with a Multiplex immunofluorescence panel of common epithelial and immune markers (Epcam, Cd4, Cd8, Foxp3 and Cd68) (Fig.46). The analysis revealed a clear increase in CD8+ cells in the epithelial compartment of ECF at day 5 versus control, but not at day 2 (Fig.46E). Furthermore, there was a decrease in the proportion of regulatory T cells with respect to the total number of T lymphocytes already by day 2 (Fig.46H).

Despite the reduction in the number of ECF, only sporadic Caspase3+ staining was observed in these samples, suggesting that ECF progenitors were not dying by apoptosis (Fig.S2). Given the influx of CD8+ cells, it was possible that immunogenic or immune-mediated forms of cell death were mediating the disappearance of ECF structures.

5.10 Gasdermin4c is profoundly upregulated in *Lgr5-Rspo3* epithelium after RXC004 treatment

Previous analysis in animal models of WNT disruption suggested a link between WNT activation and repression of the pyroptitic mediator *Gsdmc4*. Given the immunogenic

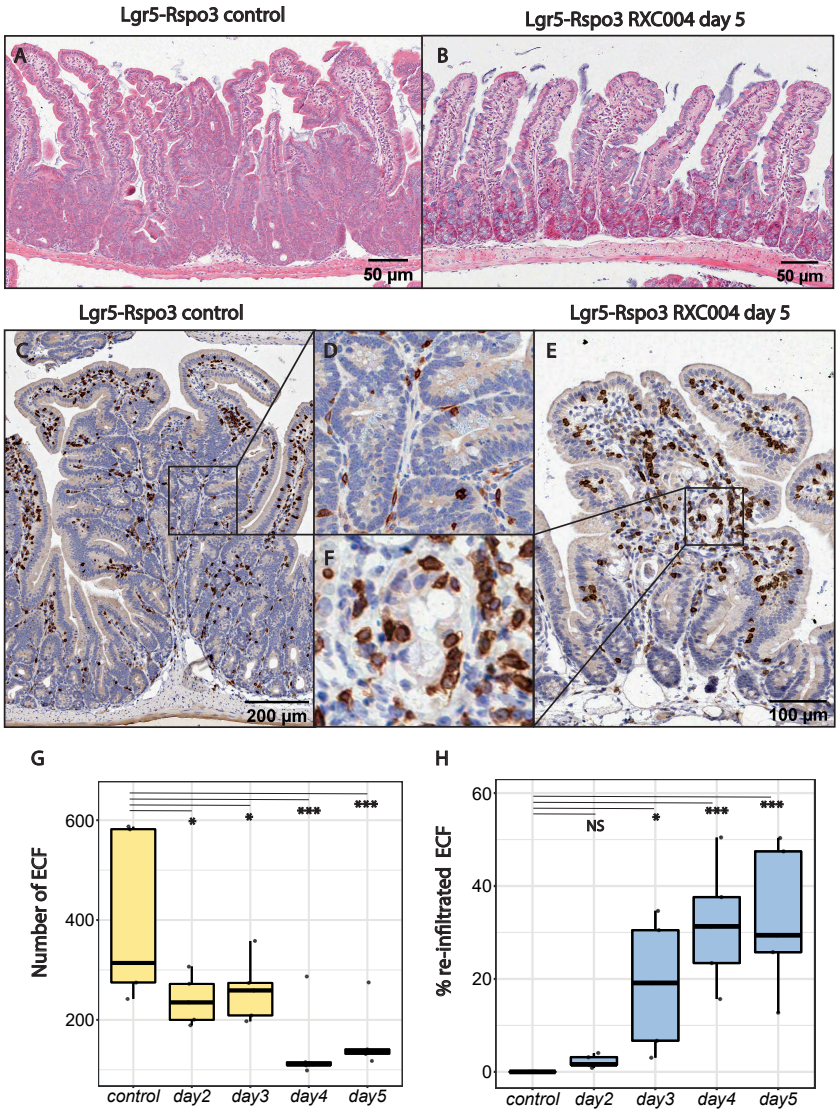

Figure 45: Treatment with a Porcupine inhibitor drives T cell infiltration in ECF from *Lgr5-Rspo3* animals. A,B. H&E of *Lgr5-Rspo3* animals treated with vehicle (A) or 1g/kg of RXC004 (B). C-E. IHC for Cd3 in polyps from *Lgr5-Rspo3* animals treated with vehicle (C,D) or 1g/kg of RXC004 (E,F). D and F show details of ECF. G-H. Quantification of the number of ECF (G) and Cd3+ cells (H) in polyps from *Lgr5-Rspo3* animals treated with vehicle or 1g/kg of RXC004. Statistical significance was assessed using a pairwise t-test and p.value was adjusted using the Holm method. Asterisks indicate a p-value <0.05 (*), <0.01(**) or <0.001 (***)

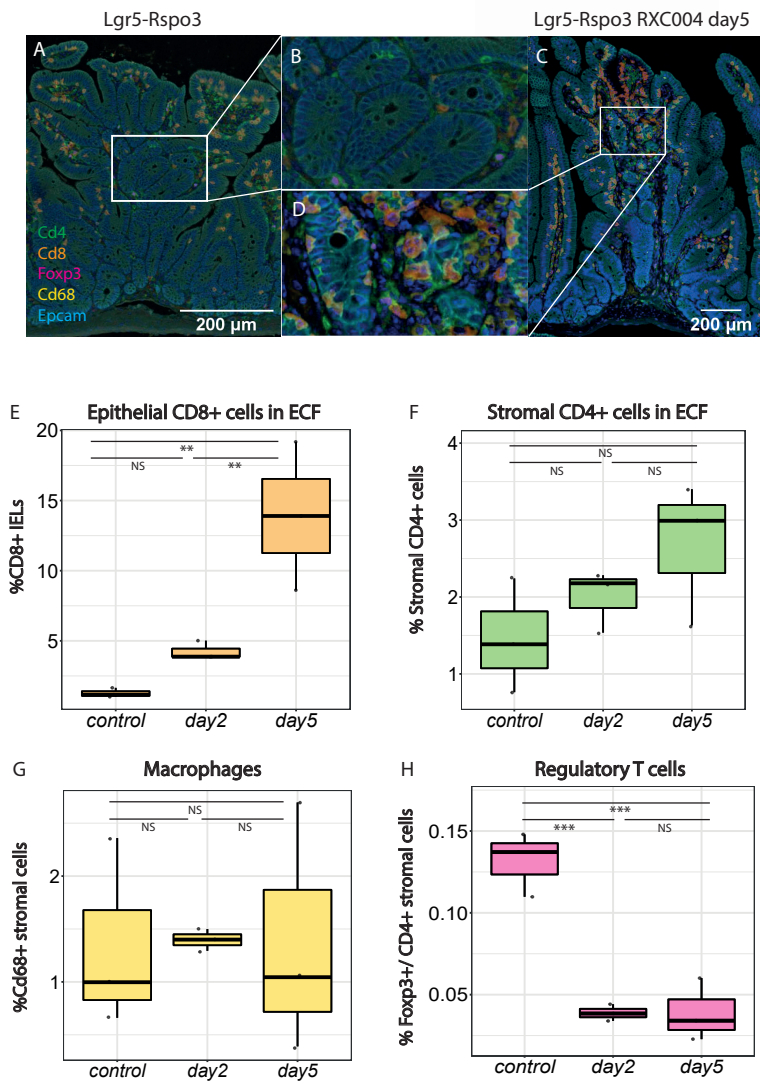

Figure 46: Treatment with a Porcupine alters the immune microenvironment within *Lgr5-Rspo3* polyps. A-D. Immune characterization of polyps from *Lgr5-Rspo3* animals treated with vehicle (A,B) or 1g/kg of RXC004 (C,D) using Multiplex Immunofluorescence (MPI) for a panel of antibodies: Cd4 (green), Cd8 (orange), Foxp3 (pink), Cd68 (yellow), Epcam (cyan), DAPI (blue). E-H. Image quantification of the numbers of Cd8+ IELs (E), Cd4+ T cells (F), Cd68+ macrophages (G) and Cd4+Foxp3+ regulatory T cells (H) in MPI images from *Lgr5-Rspo3* animals treated with vehicle or 1g/kg of RXC004. Statistical significance was assessed using a pairwise t-test and p.value was adjusted using the Holm method. Asterisks indicate a p-value <0.05 (*), <0.01(**) or <0.001 (***)

potential of this cell death mechanism, it was hypothesized that re-activation of pyroptosis could be one of the mechanisms by which abrogation of Wnt ligand was driving an immune influx into ECF from *Lgr5-Rspo3* animals. To investigate this, the expression of *Gsdmc4* was analysed in samples from treated and untreated *Lgr5-Rspo3* animals using ISH.

In WT samples, staining of this transcript was confined to the TA compartment, and stopped abruptly as cells migrated to higher positions along the villi (Fig.47A-D). In accordance with this observation, the single cell data generated by Haber et al[248] revealed that *Gsdmc4* was expressed by a population of enterocyte progenitors (Fig.S3). Regarding the distribution of this transcript across the intestine, the levels of *Gsdmc4* increased along the small bowel and reached its maximum at the colon (Fig47A-D). In sharp contrast, work by Leedham et al evidenced the physiological decrease in the levels of WNT activation along the small bowel and colon of WT animals[249]. Hence, it is plausible that these basal WNT activation levels at least partially modulate the expression of *Gsdmc4* in the murine intestine.

In agreement with previous transcriptomic analysis, the levels of *Gsdmc4* tended to decrease in the intestines of *Lgr5-Rspo3* animals, although Qupath quantification revealed that this trend was not statistically significant (Fig. 47E-H,M). However, there was a massive upregulation of this transcript upon RXC004 treatment (Fig47I-N). Interestingly, this upregulation occurred faster towards the end of the small bowel, where changes were observed only after 3 days. However, no increase in the levels of *Gsdmc4* was seen in SB1 until 4 days after treatment (Fig.47N).

It's worth noting that the temporal pattern of *Gsdmc4* upregulation matches that of the lymphocytic infiltration within ECF of RXC004-treated *Lgr5-Rspo3* mice, suggesting that there may be a mechanistic link between these two processes. Indeed, it is possible that the DAMPS and pro-inflammatory mediators generated during pyroptosis of ECF progenitors may be driving T cells into this compartment. However, further experiments are needed to validate this hypothesis.

5.10.1 *Gsdmc4* Upregulation Does not Mediate the Subtle T Cell Infiltrations Observed in *Lgr5-CreER^{ER}-DTR-APC^{Min}* Mice

To see whether the expression of *Gsdmc4* could also be linked to the limited immune infiltration observed in *Lgr5-CreER^{ER}-DTR- APC^{Min}* mice, samples of these animals were stained for *Gsdmc4*. In untransformed intestines from *APC^{Min}* controls, the pattern of expression of this transcript was comparable to that of WT animals (Fig.48A),

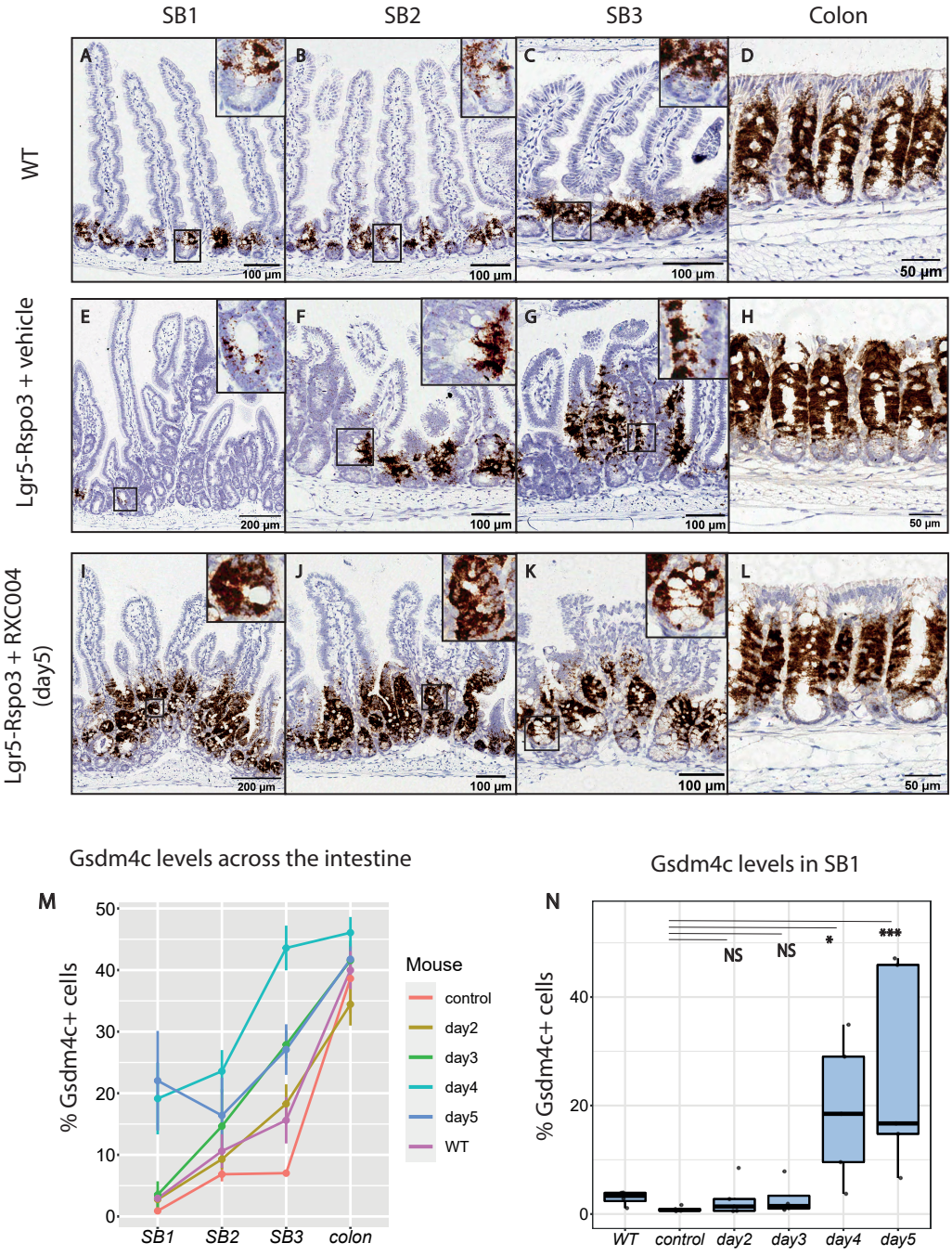

Figure 47: Treatment with a Porcupine inhibitor induces the expression of *Gsdmc4* in crypts from *Lgr5-Rspo3* animals. A-L. ISH for *Gsdmc4* in SB1(A,E,I), SB2(B,F,J) , SB3(C,G,K) or colon(D,H,L) from WT(A-D) and *Lgr5-Rspo3* animals treated with vehicle (E-H) or 1g/kg of RXC004(I-L). M,N. Quantification of the expression of *Gsdmc4* across the intestine of WT mice and *Lgr5-Rspo3* animals treated with vehicle or 1g/kg of RXC004 for 2,3,4 and 5 days. Statistical significance was assessed using a pairwise t-test and p.value was adjusted using the Holm method. Asterisks indicate a p-value <0.05 (*), <0.01(**) or <0.001 (***)

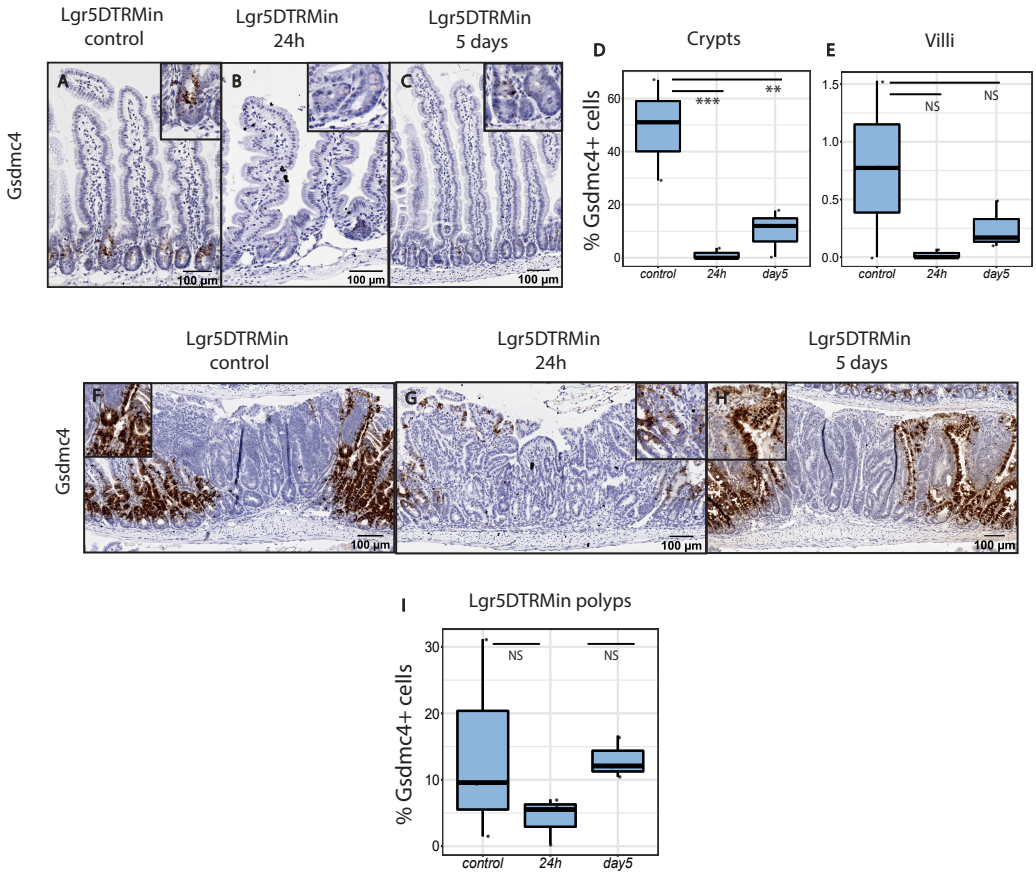

Figure 48: Administration of Diphteria Toxin (DT) to *Lgr5-CreER^{ER}-DTR- APC^{Min}* animals causes a transient downregulation of *Gsdmc4*. A-C, F-H. ISH for *Gsdmc4* in untransformed tissue (A-C) and polyps (F-H) from control and *Lgr5-CreER^{ER}-DTR-APC^{Min}* animals 24h and 5 days after DT administration. D,E,I Image quantification of the levels of *Gsdmc4+* cells in crypts (D), villi (E) and polyps (I) of controls and *Lgr5-CreER^{ER}-DTR- APC^{Min}* animals 24h and 5 days after DT administration. Statistical significance was assessed using a pairwise t-test and p.value was adjusted using the Holm method. Asterisks indicate a p-value <0.05 (*), <0.01(**) or <0.001 (***)

which was to be expected given the focalized nature of their phenotype. As observed before, DT treatment induced apoptosis of the Lgr5 compartment within 24h. At the same time, an abrupt downregulation of the *Gsdmc4* transcript was detected at the crypts compartment (Fig.48D), suggesting that DT-mediated apoptosis may dampen alternative cell death mechanisms like pyroptosis. However, the levels of *Gsdmc4* were back to normal levels by day 5 (Fig.48D), which suggest that the increase in T

cells observed in this samples was mediated by an alternative mechanism.

Overall, this data suggests a possible link between WNT inhibition and pyroptosis, which could at least partially explain the immune infiltration observed within ECF crypts of RXC-treated *Lgr5-Rspo3* mice. However, further research is needed to clarify how these two mechanisms interact, and whether they extend to other CRC models.

5.11 Discussion

Immune exclusion is one of the mechanisms by which cancers avoid immune surveillance. Despite abundant literature associating this phenomenon to WNT activation across cancers[199, 197, 194] and in the particular case of CRC[182], the mechanistic understanding of how WNT may be hindering immune recruitment to the vicinity of the tumours is still missing. In this piece of work, mouse models of WNT disruption were used to assess the correlation of WNT activation and immune exclusion and to investigate the mechanisms behind this phenomena. Furthermore, a ligand dependent model of WNT-driven polyposis was used to assess impact of pharmacological WNT inhibition on immune cell activation.

Work from Agudo et al demonstrated that quiescent SC (eg. hair follicle or smooth muscle SC) are immune privileged, meaning that they possess cell-intrinsic characteristics that render them undetectable by the immune system. However, the authors observed lymphocytic infiltration into the intestines of animals injected with activated T cells [14]. Based on this evidence, Agudo et al. concluded that, unlike quiescent SC, ISC do not possess cell-intrinsic properties that shield them from immune recognition. Nevertheless, in this study, immune phenotyping of WT animals revealed a clear decrease in immune populations and processes in CBC and TA cells versus differentiated enterocytes. In particular, a decrease in Cd8+ lymphocytes, reduced production of chemokines and antigen presenting machinery, as well as downregulation of immune processes (eg. *TCR signaling, Costimulation through the CD28 family*) were observed in homeostatic crypts. This data is in accordance with observations from Takashima et al[15], who described an uneven distribution of T cells along the crypt-villus axis of WT animals, and suggests that CBC and TA may present a relative amount of IP.

In models of WNT-driven polyposis, lesions presented reduced numbers of CD8+ cells, namely IEL, and a relative increase of Foxp3+ T lymphocytes. The neoantigens bound to the Major Histocompatibility Complex-I molecules in the surface of cancer cells are recognized by TCR in the surface of Cd8+ T lymphocytes. Within an

immune-active environment, this results in cell-mediated cytotoxicity and the consequent eradication of malignant cells. As a consequence, the levels of infiltrating Cd8+ T cells are a good prognostic factor in CRC[175, 176, 177]. Contrarily, immune suppressive Foxp3+ populations have been associated with poor clinical outcomes in the context of CRC[191]. Based on this evidence, the changes in immune populations experienced by *Lgr5-Rspo3* and APC^{Min} polyps could help them avoid immune surveillance and facilitate their progression.

The WNT-driven models of intestinal polyposis used in this study had distinct progenitor compositions: APC^{Min} polyps have a Lgr5+ CBC cell of origin (see Chapter 3), whereas *Lgr5-Rspo3* lesions are predominantly populated by Lgr5- progenitors. Despite these differences, comparable levels of immune cell infiltration were detected in these two models. Furthermore, DTR-induced killing of Lgr5+ SC did not resolve immune exclusion in APC^{Min} polyps. Collectively, these observations indicate that the immune evasion properties of a lesions are not dependant on the presence of CBC progenitors. Similarly, no differences in the immune landscape were detected between LD and LI models, suggesting that the mechanism by which WNT is disrupted does not affect the levels of immune cells that infiltrate transformed tissues, although it will impact their response to Wnt-blocking agents like RXC004.

Differences in the sensitivity to WNT inhibition were detected between WT and *Lgr5-Rspo3* mice. The reason why *Lgr5-Rspo3*, but no WT animals, experienced intestinal collapse upon treatment with the same dose of RXC004 is not clear, but it may be related to the upregulation of alternative R-spondin and Frizzled receptors (ie. *Fzd5*, *Lgr4*). Indeed, these changes may alter the levels of sensitivity to external sources of Wnt, which may render cells more susceptible to alterations in the homeostatic gradients.

Importantly, lower doses of RXC004 caused the selective infiltration of ECF by Cd8+ populations, accompanied by relative decrease in Foxp3+ T cells, which indicates a link between WNT activation and immune exclusion. In these samples, T cell infiltration was first observed 3 days after the first dose of RXC004, suggesting that WNT inhibition per se was not the direct cause of this cell influx, but additional mechanisms had to be activated before changes in the immune landscape could be observed.

Generally, the mechanism by which a cell dies can influence the immune landscape of the tissue. Pyroptosis is an immunogenic cell death mechanism that involves the production of pro-inflammatory molecules (Il-1β, Il-18) and the exposure of DAMPS[245]. *Gsdmc4* is a pyroptosis mediator which expression is normally

restricted to the TA region within homeostatic crypts. Transcriptomic analysis of WNT-disrupted animal models revealed this gene to be repressed upon WNT activation. Furthermore, Porcupine inhibition resulted in a significant upregulation of *Gsdmc4* in *Lgr5-Rspo3* intestines, more precisely within the hyper-proliferative and ECF compartments. Importantly, the timing of *Gsdmc4* upregulation matched that of the T cell infiltration into ECF, suggesting that these phenomena may be related. It is possible that pyroptosis plays an active part in the recruitment of immune cells. Alternatively, pyroptosis could be a mechanisms of immune-mediated cell clearance. Further research is needed to clarify the exact role that *Gsdmc4* plays in the RXC004-driven immune changes observed in *Lgr5-Rspo3* polyps.

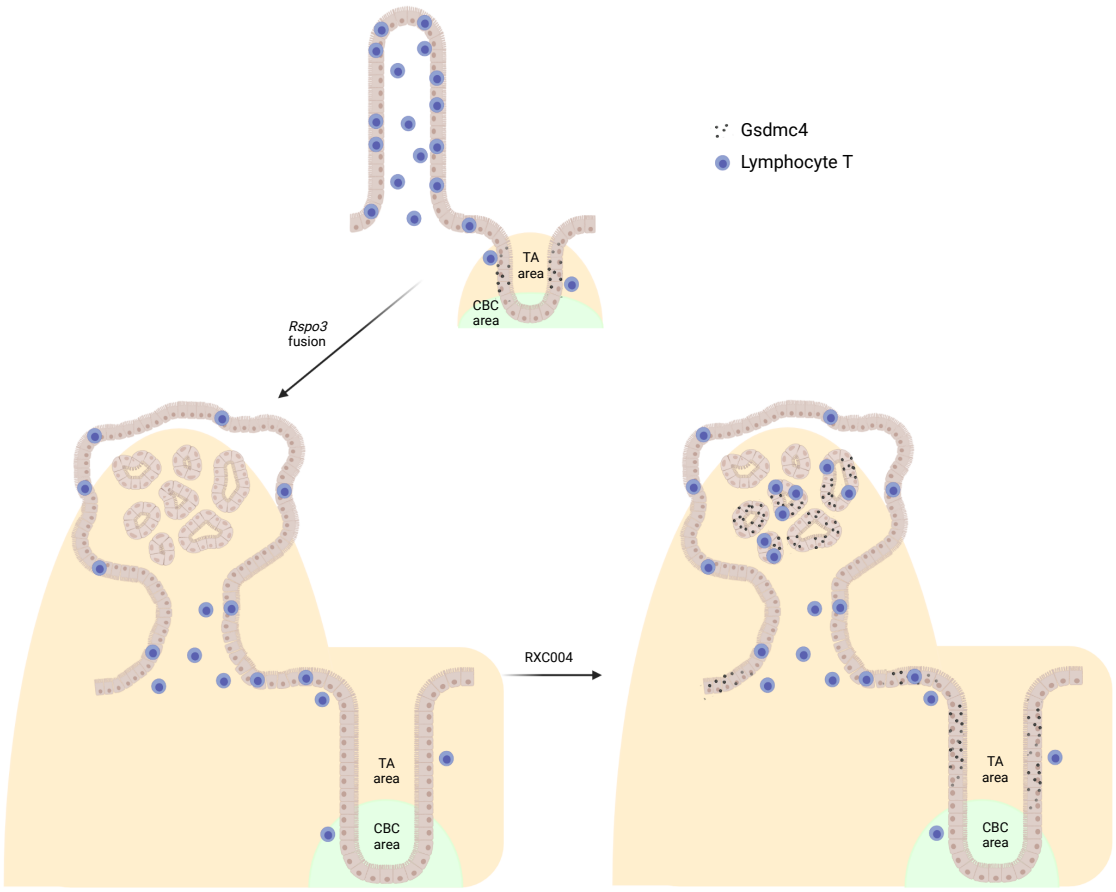

Figure 49: Treatment with a Porcupine inhibitor drives re-infiltration of T lymphocytes into the ECF from Lgr5-Rspo3 animals.

Unlike ECF, conventional crypts within RXC004-treated *Lgr5-Rspo3* animals retained their normal-looking, immune-excluded structure. I hypothesize that the different sensitivity of conventional and ectopic crypts may derive from their distinct cell composition. The Lgr5- cells from which ECF originated had a baseline expression of *Gsdmc4*, which may increase their susceptibility to death by pyroptosis upon WNT inhibition, whereas CBC require higher doses of the drug for their integrity to be compromised.

Unlike immunogenic forms of cell death (e.g. pyroptosis, necroptosis), which propitiate the activation of an immune response against the tumour, silent modalities of cell clearance facilitate immune evasion and cancer progression[195]. In this line, DTR-mediated apoptosis had no effects in the immune recruitment towards APC^{Min}-$Lgr5^{DTR}$ polyps. Interestingly, activation of apoptosis in Lgr5+ progenitors drove the downregulation of *Gsdmc4*, suggesting that cell death mechanisms may co-exist in an equilibrium, although the nature of this balance requires further study.

Based on the results presented in this chapter, I propose a mechanisms by which WNT activation may be driving immune exclusion, which is summarized in the following hypothesis (Fig.49): there is a predilection for different forms of programmed cell death along the crypt-villus axis. At the crypts, CBC cells express anti-apoptotic proteins [84], and keep a low expression of pyroptotic genes. However, selective expression of *Gsdmc4* suggests that pyroptosis may be active within the TA compartments. This may help prevent the accumulation of mutations which result from their highly proliferative activity by limiting their life-span. In ligand-dependent models of WNT-driven transformation, like the *Lgr5-Rspo3* mouse, preferential expansion of Lgr5- progenitors within the TA compartment drives the development of polyps and ECF. In this context, WNT activation may suppress pyroptosis, at least partially through repression of pyroptotic effectors (i.e. *Gsdmc4*). Consequently, abrupt abrogation of the Wnt ligand drive may reactivate this mechanism, which would cause the observed influx of T lymphocytes. However, whether pyroptosis activation could facilitate T cell infiltration into lesions driven by alternative progenitor populations, like APC^{Min} polyps, remains to be determined.

The vast array of mechanisms by which WNT may be mediating immune exclusion across CRC malignancies is far from being comprehended. Nevertheless, this work proposes a mechanisms by which immune-exclusion may be mediated in ligand-dependent models of CRC. Importantly, LD malignancies (e.g. Rspo3-driven lesions) may respond to low doses of Porcupine inhibitors, which might help limit the noxious

side-effects associated to WNT inhibition. Indeed, Porcupine inhibitors could work well in tandem with immunotherapy to drive immune-mediated clearance.